Journal of Insect Science, (2018) 18(5): 20; 1–7
doi: 10.1093/jisesa/iey106
Research

Characterization of Sphingomyelin Phosphodiesterase Expression in Bumblebee (*Bombus lantschouensis*)

Lei Han, Guiling Ding, Yanjie Liu, Jiaxing Huang,[1] and Jie Wu

Key Laboratory of Insect-Pollinator Biology of the Ministry of Agriculture, Institute of Apicultural Research, Chinese Academy of Agricultural Sciences, No. 1 Beigou, Xiangshan, Haidian District, Beijing 100093, China and [1]Corresponding author, e-mail: huangjiaxing@caas.cn

Subject Editor: Guy Bloch

Received 2 August 2018; Editorial decision 30 September 2018

Abstract

Sphingomyelin phosphodiesterase (*SMPD*) is a hydrolase that plays a major role in metabolic reactions involving sphingomyelin. Here, we describe an analysis of the cDNA sequence and gene structure of *SMPD* in bumblebee (*Bombus lantschouensis*). The expression of *SMPD* in different tissues and at different developmental stages and reproductive statuses was examined by real-time polymerase chain reaction (PCR). The results showed that the *SMPD* cDNA has a length of 2000 bp and contains an open reading frame (ORF) of 1,801 nucleotides that encodes a polypeptide of 599 amino acids. The full-length *SMPD* gene is 4228 bp and contains eight exons and seven introns. A comparative analysis revealed that the *SMPD* gene sequence in *B. lantschouensis* shares high sequence identity with those in other *Bombus* species. The *SMPD* gene is expressed broadly in various tissues and presents higher transcript levels in the ovary, midgut, and epidermis and thoracic tissues. Among the different developmental stages, the highest expression of *SMPD* was detected at the Pw pupal stage (pupae with an unpigmented body cuticle and white eyes), and the expression of this gene decreased from the Pp (pupae with pink eyes) to the Pdd (dark-eye pupae with a dark-pigmented cuticle) stages. In addition, *SMPD* expression was significantly upregulated after female egg laying. In conclusion, our results show that the bumblebee *SMPD* gene might play a key role at the Pw developmental stage and in female oviposition.

Key words: bumblebee, *Bombus lantschouensis*, Sphingomyelin phosphodiesterase, cloning, gene expression

Sphingomyelin phosphodiesterase (*SMPD*) is a hydrolytic enzyme involved in sphingolipid-related metabolic reactions. These reactions hydrolyze the conversion of sphingomyelin to phosphocholine and ceramide, which play important roles in signal transduction (Kanfer et al. 1966, Hofmann et al. 2000, Ago et al. 2006, Kramer et al. 2015, Lim et al. 2016). *SMPD* was first identified in fibroblasts from patients with Niemann-Pick disease (NPD) (Schneider and Kennedy 1967). Subsequent reports have demonstrated that *SMPD* can inhibit forms of colorectal carcinoma and colitis (Hertervig et al. 1998, Sjöqvist et al. 2002, Hertervig et al. 2015). Furthermore, ceramide, which is produced by a reaction catalyzed by sphingomyelinase (SMase), inhibits cellular signaling events downstream of insulin signaling and ultimately affects diabetes (Deevska et al. 2009). Despite the interesting effects of *SMPD* in humans, limited studies have characterized this protein in insects (Renault et al. 2002, Han et al. 2017). In this study, we sought to explore the characteristic molecular expression of *SMPD* in the bumblebee, which represents an important pollinator of wild plants and crops.

SMase is classified as aSMase (pH: 4.5~5), nSMase (pH: ~7) or alSMase (pH~9) according to its cation dependence and the pH required for its optimal activity. Studies have indicated that an increased level of aSMase can accelerate the risk of apoptosis-induced myocardial infarction (O'Brien et al. 2003), and aSMase activity is important for sperm maturation and function (Butler et al. 2002). In insects, five homologs of *SMPD* genes are widely expressed in *Drosophila* embryos (Renault et al. 2002). A microarray study revealed that an acid SMase and fatty acid synthesis are downregulated and upregulated, respectively, after sugar feeding, which indicates that the product of SMase might play an important role in downregulating fatty acid synthesis (Zinke et al. 2002). Five sequences of SMases have been identified in the tsetse fly genome. Moreover, the expression of aSMase1 reportedly increases by approximately 1000-fold during pregnancy and the gonotrophic cycle, and RNAi knockdown of aSMase1 in tsetse flies greatly extends larval development and affects offspring health (Benoit et al. 2012).

The bumblebee (*Bombus lantschouensis* Vogt) is a polylectic and primitively eusocial bee that plays a key role in the pollination of wild plants and crops in North China (An et al. 2014) and represents an excellent native species that is often selected for artificial rearing and greenhouse crop pollination in China (Wu et al. 2007, 2009; An et al. 2010). Our previous differential proteomics analysis of female

B. lantschouensis showed that *SMPD* exhibits marked differential expression in the hemolymph plasma of female bumblebees at different reproductive stages. Therefore, understanding the spatiotemporal characteristics of *SMPD* gene expression in the bumblebee could provide insights into its functions.

In this study, we cloned the full-length cDNA sequence of the *SMPD* gene in *B. lantschouensis* and determined its expression in different tissues and at different developmental stages as well as its relationship with different reproductive statuses. The 3D structure of the *SMPD* protein was also predicted. The results of this study provide basic knowledge regarding the mechanism underlying the regulation of *SMPD* expression in bumblebee.

Materials and Methods

Sample Collection

Colonies of *B. lantschouensis* were initiated using queens collected on April 2015 from Lanzhou, Gansu Province, China. The colonies were maintained in a breeding room at 28 ± 2°C with 60 ± 10% RH, and pollen and 50% sugar solution were provided ad libitum (Yong et al. 2003). Eighteen egg-laying queens were dissected on ice with a stereomicroscope (SZX16, Olympus, Japan), and the antenna (AN), head (HD), thorax (TH), midgut (MG), leg (LG), venom gland (VG), ovary (OV), fat body (FB), and epidermis (EP) from each bumblebee were collected. The tissues from six bees used as biological replicates were pooled, and total RNA was extracted. Samples from three bumblebee workers at each developmental stage, with the exception of the egg stage, were obtained individually at the following stages: within 48 h of larval hatching (Lar), pupae with an unpigmented body cuticle and white eyes (Pw), pink eyes (Pp), and brown eyes (Pb), pupae with dark brown eyes and a light-pigmented thorax (Pbl), and pupae with brown eyes and a dark-pigmented cuticle (Pbd). Eighteen eggs (egg) were sampled within 24 h of laying and randomly divided into three biological replicates (six eggs in each replicate). Three egg-laying and non-egg-laying queens/workers were collected to measure the expression level of the *SMPD* gene at different reproductive statuses, and the reproductive statuses (egg-laying vs. non-egg-laying) of the workers and queens were determined based on the development of their ovaries (Duchateau and Velthuis 1989). All the samples were frozen in liquid nitrogen until use.

RNA Extraction and Amplification of Full-Length cDNA

Total RNA from all the samples was extracted using TRIzol (Invitrogen, Carlsbad, CA) following the manufacturer's instructions. The integrity of the isolated RNA was checked by 1.5% (w/v) agarose gel electrophoresis. The concentration and quality of the extracted RNA were estimated based on the A260/280 ratio, which was measured using a NanoDrop 2000 spectrophotometer (Thermo Fisher Scientific, Waltham, MA). Full-length cDNA was amplified using the SMARTer rapid amplification of cDNA ends (RACE) amplification kit (Clontech, Mountain View, CA). The primers SMPD934-F and SMPD992-R (Table 1) were designed based on the predicted sequence of the *SMPD* gene in *Bombus terrestris* (*XM_003401974*) for 5′ and 3′ RACE, respectively. The following conditions were used for the polymerase chain reaction (PCR) assay: five cycles of 94°C for 30 s and 72°C for 2 min, five cycles of 94°C for 30 s, 70°C for 30 s and 72°C for 2 min, and five cycles of 94°C for 30 s, 68°C for 30 s and 72°C for 2 min. All the amplification products were separated on a 1.0% agarose gel. After purification, the PCR products from the right size were ligated into a $p^{MD19\text{-}T}$ Vector (Takara Bio Inc., Dalian, China) and transformed into Trans1-T1 competent cells (TransGen Biotech, Beijing, China). Positive colonies were sent for sequencing by the SinoGenoMax Company (Beijing, China). The full-length cDNA sequences of *SMPD* were derived by assembling the obtained 5′- and 3′-end sequences.

Genomic DNA Extraction and *SMPD* Gene Sequence Amplification

Genomic DNA was extracted using a Wizard Genomic DNA purification kit (Promega, Madison, WI, USA). Three pairs of primers, SMPDU-F + SMPD779-R, SMPD338-F + SMPD992-R and SMPD934-F + SMPDU-R (Table 1), were designed based on the obtained *SMPD* cDNA sequence of *B. lantschouensis*. The complete *SMPD* gene was assembled based on the cloned and sequenced PCR products obtained using the above-mentioned primers.

Sequence Analysis

Homologous sequences to the *SMPD* gene in *B. lantschouensis* were identified through an NCBI nucleotide BLAST search, and data for *Apis cerana* (XP 016915509), *Apis mellifera* (XP 016769255), *Apis dorsata* (XP 006608650), *Apis florea* (XP 012341557), *B. terrestris*

Table 1. Primers used in this study

Purpose	Name	Primer sequence (5′–3′)	Annealing temperature (°C)	Amplicon length (bp)
3′ RACE	SMPD934-F	CAGTTCGCACCAAAAAATATAACGCAAGACA	72	-
5′ RACE	SMPD992-R	AATTTATAAAGCCAATTTGTAGTTAAATTGTCTTGCGT	72	-
GENE	SMPDU-F	ATGTGGTTTCAACAATTAATTTTG	53	2178
	SMPD779-R	CATGCCATGGGGTATCACAGGAG		
	SMPD338-F	TCCAAACCGAAAGAGTTTGTAG	55	1282
	SMPD992-R	CAATTTGTAGTTAAATTGTCTTGCGT		
	SMPD934-F	CAGTTCGCACCAAAAAATATAACGC	55	1290
	SMPDU-R	TCAATTCTTTAAAATATTATTACATAGTTC		
Real-time PCR	SMPDF-F	AATGGCAGACCTATGGATTGTATATGGAT	60	186
	SMPDF-R	TGTAGTTGATTATCAGGATCTTGCGGATTA		
	β-actin-F	CGACTACCTCATGAAGATT	60	101
	β-actin-R	CGACGTAACAAAGTTTCTC		
	GAPDH-F	GCTGGAGCTGAATATGTTGTAGAATC	60	195
	GAPDH-R	AGTAGTGCAGGAAGCATTAGAGATAACT		

(XP 003402022), *Bombus impatiens* (XP 012246958), and *Nasonia vitripennis* (XP 008213818) were downloaded. All the sequences were edited and aligned using BioEdit version 7.2.5 (Hall 1999). A phylogenetic tree was constructed using MEGA version 7.0.26 (Tamura et al. 2013). The best protein model was selected using the model selection function in MEGA software, and based on AIC values, the best model was mtREV24. The maximum parsimony (MP) and neighbor-joining (NJ) methods with 1,000 bootstrap replicates were adopted. The signal peptide motif of the coding protein sequence of *SMPD* was predicted using SignalP 4.0 (Petersen et al. 2011), and the molecular weight and isoelectric points (pIs) were estimated using ProtParam (Gasteiger 2005). The predicted three-dimensional (3D) crystal structure of *SMPD* was obtained from the Swiss-Model server (https://swissmodel.expasy.org/) (Biasini et al. 2014), and human acid SMase from the Protein Data Bank (ID: 5i81) was used as the 3D crystal template. The model result was evaluated based on Qualitative Model Energy Analysis (QMEAN) and Global Model Quality Estimation (GMQE) values. QMEAN is a composite scoring function describing the major geometrical aspects of protein structures (Schomburg 2010). QMEAN Z-scores around zero indicate good agreement between the model structure and experimental structures of similar size, whereas scores of –4.0 or below indicate that the models is of low quality (Benkert et al. 2011). GMQE is a quality estimation method that combines properties from the target-template alignment and template search methods. The GMQE score is expressed as a number between 0 and 1, with higher numbers indicating greater reliability (Waterhouse et al. 2018). The binding confirmation was displayed using PyMOL (http://www.pymol.org/pymol).

Expression Analysis Using Real-Time Quantitative PCR

The mRNA expression profiles of *SMPD* in different tissues and at different developmental stages and the relationship of *SMPD* with the reproductive status of workers and queens were examined by real-time quantitative PCR. Total RNA was extracted, and first-strand cDNA was generated using the PrimeScript First-strand cDNA Synthesis kit (Takara Bio Inc., Dalian, China) following the manufacturer's instructions. Real-time PCR was performed using the SYBR Premix ExTaq II kit (Takara, Dalian, China) and a Stratagene Mx3000 real-time PCR system (Agilent, United States). The primers SMPDF-F and SMPDF-R were designed based on the full-length sequence of *SMPD* obtained from the RACE-PCR analysis. The expression of β-actin and GAPDH transcripts, which were used as endogenous controls, was assessed using the primers β-actin-F/R and GAPDH-F/R (Table 1). The amplification conditions were as follows: 95°C for 30 s followed by 40 cycles of 95°C for 5 s and 60°C for 30 s. Each sample was replicated three times, and relative *SMPD* expression levels were quantified using the comparative $2^{-\Delta\Delta Ct}$ method (Livak and Schmittgen 2001). One-way analysis of variance (ANOVA) was applied using R-Project software (version 3.3.2) to assess the differences in expression level between different reproductive statuses ($P < 0.05$).

Results

Full-Length cDNA and Sequence Analysis of *SMPD*

The full-length *SMPD* cDNA sequence is 2000 bp. The 5′ and 3′ untranslated regions (UTR) are 58 and 141 bp, respectively, and the 3′ UTR contains the polyadenylation signal (AATAAA) (GenBank accession number: MH594210) (Fig. 1). The hypothetical ORF of 1,800 nucleotides is predicted to encode a protein consisting of 599 amino acids. The initiation (ATG) and stop codons (TGA) in the ORF were found at 59 and 1856 bp in the cDNA sequence, which suggests that this sequence contains the complete coding region. The predicted molecular weight and theoretical pI of *SMPD* are 69.91 kDa and 5.76, respectively. A 17-aa signal peptide at the beginning of the *SMPD* amino acid sequence was identified using the SignalP 4.1 server. Genomic amplicon sequencing showed that the length of the *SMPD* gene is 4228 bp, and an analysis of the gene structure revealed that it contains eight exons and seven introns (Fig. 1).

Protein Sequence Alignment and Phylogenetic Analysis

According to the predicted *SMPD* amino acid sequence, the length of the mature peptide is 580 aa. The mature protein sequence was aligned with multiple sequences (included in GenBank) from bees that are predicted to exhibit a close evolutionary relationship, and the alignment showed that the protein is highly conserved within the Apidae family. A multiple-sequence alignment demonstrated that the *SMPD* protein from *B. lantschouensis* exhibited the typical features of the MPP and SapB_2 superfamilies, including a saposin B domain (residues 60–132), calcineurin-like phosphoesterase domains (222–289) and a metallophosphatase (MPP) domain (170–468) (Fig. 2). Moreover, the conserved MPP domain was found to contain eight putative active sites and seven putative metal-binding sites.

The comparison of the deduced mature amino acid sequences also indicated that the *SMPD* gene in *B. lantschouensis* is closely related to homologous genes found in other bees (97.1 and 99.7% similarity to *B. terrestris* and *B. impatiens*, respectively, and 75.2–78.7% similarity to *A. cerana*, *A. florea*, *A. dorsata,* and *A. mellifera*). The phylogenetic tree constructed based on the obtained identity values reflected a relationship among the selected insects. If

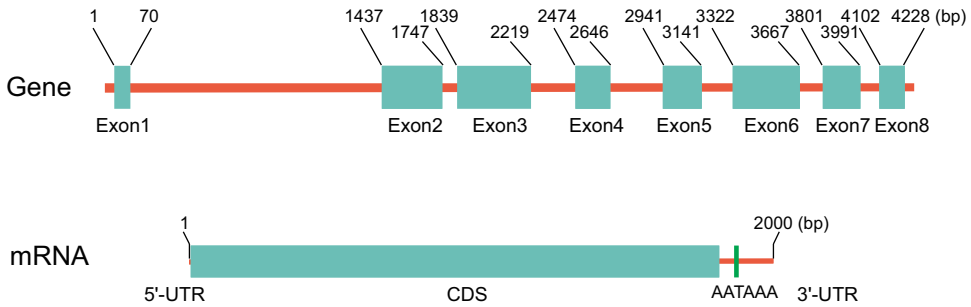

Fig. 1. Gene structure of *SMPD* in bumblebee (*Bombus lantschouensis*). (A) Gene structure of *SMPD*. (B) mRNA structure of *SMPD*. The numbers indicate the position in the sequence. A polyadenylation signal (AATAAA) is found at the end of the mRNA sequence.

N. vitripennis was considered an outlier, bumblebees and honeybees were grouped into two clusters (Fig. 3A and B).

Structure of *B. lantschouensis SMPD*

The tertiary structures of *B. lantschouensis SMPD* protein were modeled based on the structure (PDB ID: 5i81 chain A) of human acid SMase. The sequence identity between the target and template proteins was more than 30% (31.64%), and the QMEAN and GMQE values were –0.32 and 0.62, respectively, which indicated that the modelled structure was feasible. The structure analysis showed that the overall structure consisted of three functional domains, i.e., the Sap, phosphatase and C-term domains. Eight α helixes formed two functional domains at the surface of *SMPD*, and each functional domain contained four α helixes (Fig. 4A). Similar to other *SMPD* structures, the *SMPD* protein functional center in *B. lantschouensis* consisted of six α helixes (α1, α2, α3, α4, α5 and α6) and 12 β sheets (β1, β2, β3, β4, β5, β6, β7, β8, β9, β10, β11 and β12) (Fig. 4A), and

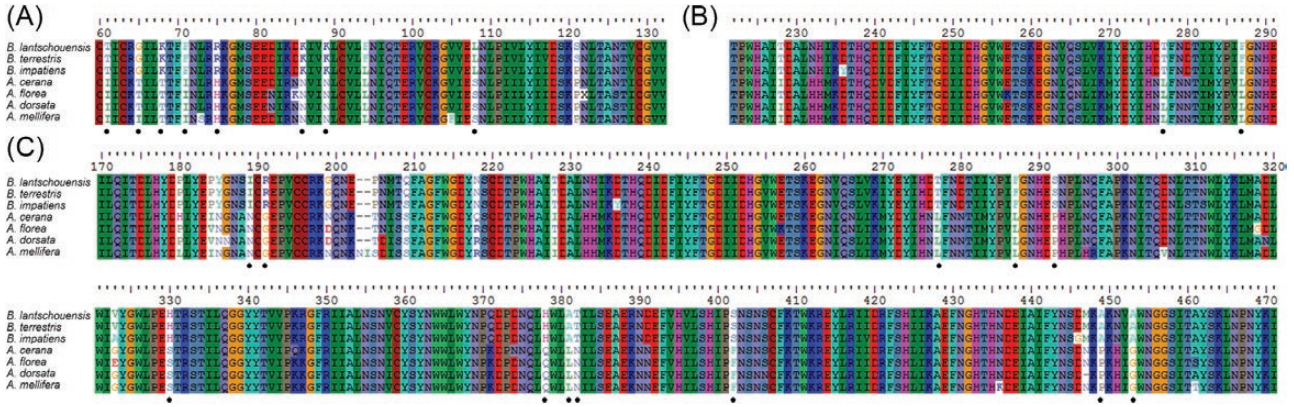

Fig. 2. Comparison of the amino acid sequences of three conserved domains in *B. lantschouensis SMPD* with those in other orthologs. (A) Saposin B domain, (B) MPP domains, and (C) calcineurin-like phosphoesterase domain. The non-conserved residues between *Bombus* and *Apis* is indicated by dots (.).

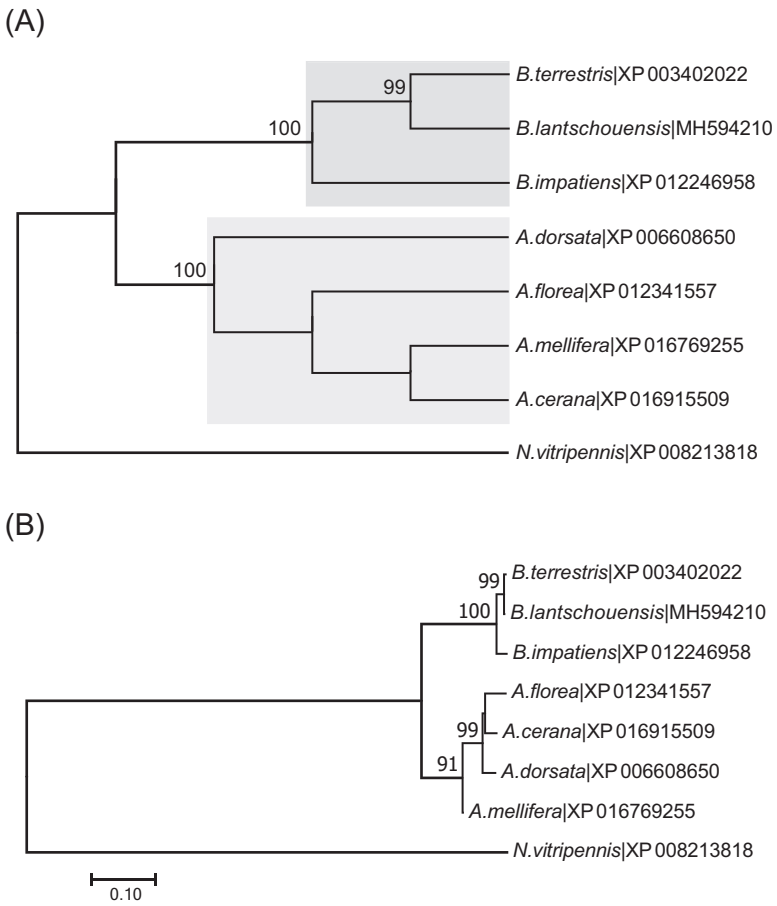

Fig. 3. (A) MP tree based on multiple *SMPD* protein sequences constructed using MEGA7. The MP tree was obtained using the Subtree-Pruning-Regrafting (SPR) algorithm with bootstrap values of 1,000 replicates. (B) The evolutionary history of the *SMPD* protein was inferred using the neighbor-joining method in MEGA7. The percentage of replicate trees in which the associated taxa clustered together in the bootstrap test (1,000 replicates) is shown next to the branches.

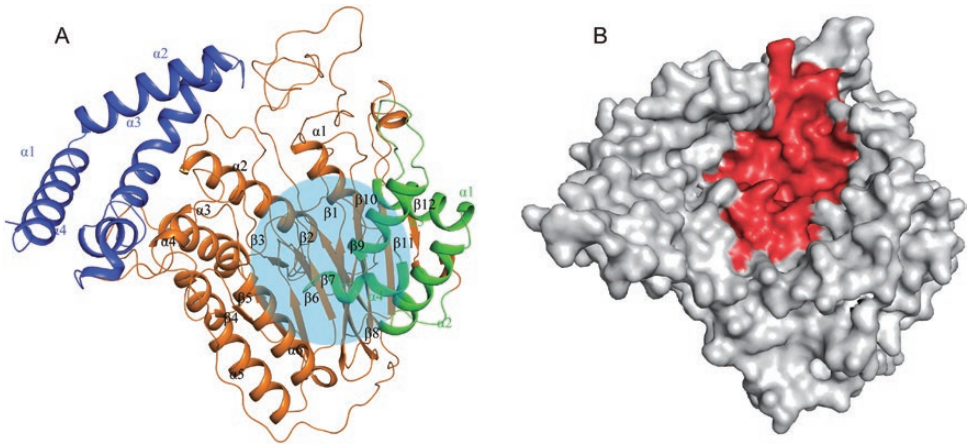

Fig. 4. Modelled tertiary structures of the *B. lantschouensis SMPD* protein based on the template of human acid sphingomyelinase (PDB ID: 5i81 chain A).

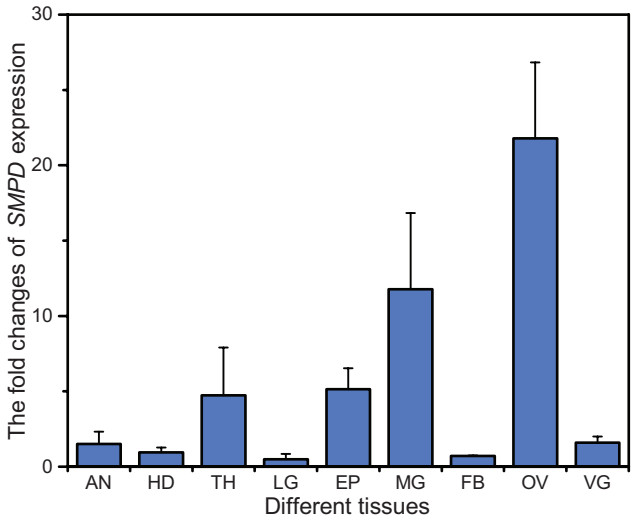

Fig. 5. Analysis of relative *SMPD* expression in different tissues of bumblebee (*B. lantschouensis*). Antenna (AN), midgut (MG), leg (LG), head (HD), venom gland (VG), ovary (OV), thorax (TH), fat body (FB), and epidermis (EP).

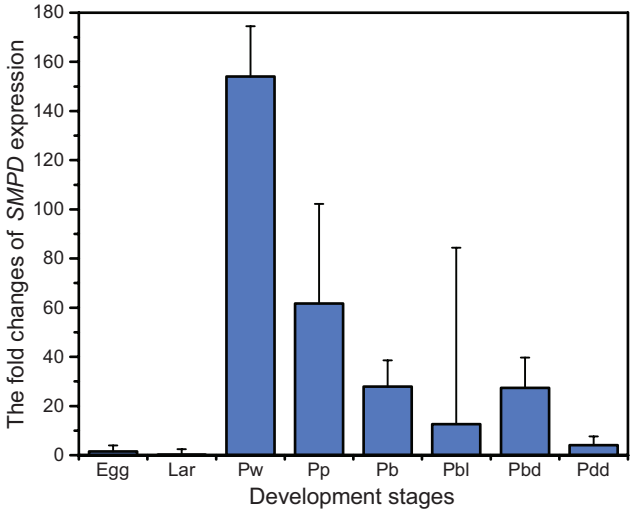

Fig. 6. Analysis of the relative *SMPD* expression at different developmental stages of bumblebee (*B. lantschouensis*). Egg (within 24 h of laying), Lar (within 48 h of hatching), Pw (white-eyed pupae with an unpigmented cuticle), Pp (pink-eyed pupae with an unpigmented cuticle), Pb (brown-eyed pupae with an unpigmented cuticle), Pbl (brown-eyed pupae with thoracic pigmentation), Pbd (brown-eyed pupae with a dark-pigmented cuticle) and Pdd (dark-eye pupae with a dark-pigmented cuticle).

the β sheets formed the enzyme catalytic activity center, which represents the binding site for sphingomyelin (Fig. 4B).

Expression Patterns of *SMPD* mRNA in Different Tissues and at Different Developmental Stages and the Relationship of *SMPD* to Reproductive Status

The expression of *SMPD* mRNA was examined in all bumblebee tissues. Higher levels of expression were detected in the OV, MG, EP, and TH, whereas significantly lower levels of expression were observed in the FB, HD, and LG ($P < 0.05$; Fig. 5). Variable levels of *SMPD* mRNA expression were observed during the development of bumblebee workers, with higher transcript levels in pupae compared with eggs and larvae. The highest expression level was observed at the Pw stage, and transcript expression continuously decreased thereafter (Fig. 6). The analysis of the workers and queens with different reproductive statuses (egg-laying vs. non-egg-laying) revealed significantly higher expression levels in the egg-laying females, and *SMPD* mRNA was significantly upregulated in egg-laying queens and workers compared with non-egg-laying queens and workers ($P < 0.01$; Fig. 7). This result indicated that *SMPD* is positively correlated with an enhanced female reproductive status.

Discussion

The *SMPD* gene is associated with diseases in humans and plays a key role in cell apoptosis in mammals (Schneider and Kennedy 1967, Hofmann et al. 2000, O'Brien et al. 2003, Duan et al. 2007), but few studies have focused on *SMPD* in insects (Renault et al. 2002, Benoit et al. 2012, Han et al. 2017). *SMPD* represents a candidate gene that has been identified in different proteomics analyses of egg-laying and non-egg-laying female bumblebees. In this study, the full-length cDNA sequence and structure of the *SMPD* gene in this important pollinator was clarified for the first time. Additionally, the *SMPD* expression profiles in different tissues and at different developmental stages and reproductive statuses were assessed.

This study revealed that *SMPD* contains many exons and introns and has two conserved domains, a saposin B domain and a MPP domain, which are representative domains observed in the *SMPD* gene superfamily. Saposin B is a small lysosomal protein that acts as an activator of various lysosomal lipid-degrading enzymes (Christomanou et al. 1986, Li et al. 1988, Munford et al. 1995) and

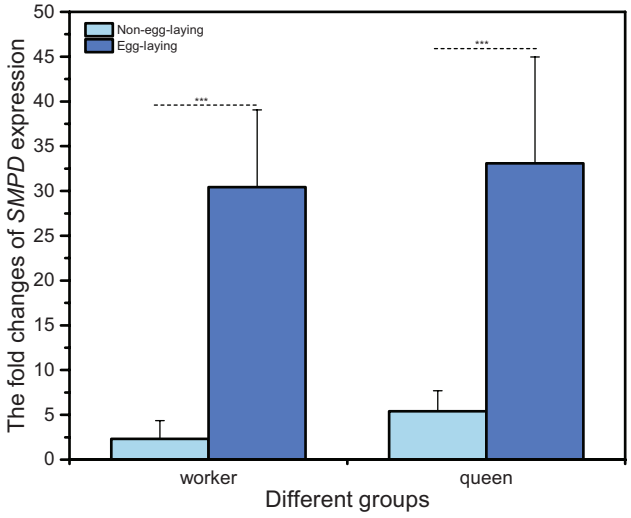

Fig. 7. Different expression of the *SMPD* gene in *B. lantschouensis* queens and workers at different reproductive stages. The asterisk above the error bar indicates that the expression level was significantly different ($P < 0.01$).

plays an important role in membrane lysis (Ponting 1994). The MPP domain contains the enzyme's active site, which is a β-sheet located at the C terminus that interacts with two metal ions (usually manganese, iron, or zinc) coordinated with histidine, aspartate and asparagine residues (Williams 2004, Matange et al. 2015).

Our results showed that the *SMPD* transcript level was more than 150-fold higher at the Pw pupae stage than at the 48-h larval stage. However, high levels of the protein were found at the egg and larvae stages (Han et al. 2017). The *SMPD* expression level decreased significantly after the Pw pupae stage, which is consistent with our previous findings regarding the expression of this protein (Han et al. 2017). Therefore, the function of *SMPD* is more important during the Pw developmental stage than during the larvae and other pupae developmental stages. Similar results were obtained in *Drosophila* embryos (Renault et al. 2002). The tissue-specific expression levels demonstrated that *SMPD* was expressed in all tissues, similarly to its expression in mammals. Among the bumblebee tissues, the ovary exhibited the highest expression of this protein, which was consistent with the higher expression detected in egg-laying female bumblebees. However, high expression levels of *SMPD* in the mammalian head and brain have also been reported (Rao and Spence 1976, Liu et al. 1998, Goni and Alonso 2002).

The expression of *SMPD* transcripts in female *B. lantschouensis* was upregulated significantly during egg laying compared with that detected in bumblebees with a non-egg-laying status. This finding confirmed the results from our proteomic analysis, which revealed that *SMPD* shows differential expression in the female bumblebee according to the reproductive status. It has been demonstrated that the knockdown of *SMPD* in tsetse flies by short-interfering RNA reduces the fecundity of adult progeny (Benoit et al. 2012). Therefore, *SMPD* is considered to be related to bumblebee reproduction. This study examined only the expression changes at different egg-laying statuses, and no further validation was performed because a mature transgenic system for bumblebees has not yet been developed. Despite its preliminary nature, this study clearly indicates that *SMPD* plays an important role in female egg laying and pupal development in bumblebee.

Conclusions

In summary, the study provides the first characterization of the full-length cDNA and gene sequence of the bumblebee *SMPD*, and the genetic phylogeny and tertiary structure of *SMPD* were predicted. Furthermore, our results demonstrated that *SMPD* might play important roles during the Pw pupal developmental stage and might affect the female egg-laying status. Tissue expression detection confirmed that *SMPD* is largely expressed in the epidermis and fat body. Therefore, the results of the present study provide basic knowledge of the bumblebee *SMPD* gene.

Acknowledgments

We thank Dr. Tolera Kumsa Gemeda for his comments and revisions. This work was supported by the China Agriculture Research System (CARS-44), the Agricultural Science and Technology Innovation Program (CAAS-ASTIP-2018-IAR) and the National Natural Science Foundation of China (U1603108).

References Cited

Ago, H., M. Oda, M. Takahashi, H. Tsuge, S. Ochi, N. Katunuma, M. Miyano, and J. Sakurai. 2006. Structural basis of the sphingomyelin phosphodiesterase activity in neutral sphingomyelinase from *Bacillus cereus*. J. Biol. Chem. 281: 16157–16167.

An, J. D., J. X. Huang, P. H. Williams, J. Wu, and B. F. Zhou. 2010. Species diversity and colony characteristics of bumblebees in the Hebei region of North China. Chin. J. Appl. Ecol. 21: 1542–1550.

An, J., J. Huang, Y. Shao, S. Zhang, B. Wang, X. Liu, J. Wu, and P. H. Williams. 2014. The bumblebees of North China (Apidae, Bombus Latreille). Zootaxa. 3830: 1–89.

Benkert, P., M. Biasini, and T. Schwede. 2011. Toward the estimation of the absolute quality of individual protein structure models. Bioinformatics. 27: 343–350.

Benoit, J. B., G. M. Attardo, V. Michalkova, P. Takac, J. Bohova, and S. Aksoy. 2012. Sphingomyelinase activity in mother's milk is essential for juvenile development: a case from lactating tsetse flies. Biol. Reprod. 87: 1–10.

Biasini, M., S. Bienert, A. Waterhouse, K. Arnold, G. Studer, T. Schmidt, F. Kiefer, T. Gallo Cassarino, M. Bertoni, L. Bordoli, et al. 2014. SWISS-MODEL: modelling protein tertiary and quaternary structure using evolutionary information. Nucleic Acids Res. 42: W252–W258.

Butler, A., X. He, R. E. Gordon, H. S. Wu, S. Gatt, and E. H. Schuchman. 2002. Reproductive pathology and sperm physiology in acid sphingomyelinase-deficient mice. Am. J. Pathol. 161: 1061–1075.

Christomanou, H., A. Aignesberger, and R. P. Linke. 1986. Immunochemical characterization of two activator proteins stimulating enzymic sphingomyelin degradation in vitro. Absence of one of them in a human Gaucher disease variant. Biol. Chem. Hoppe. Seyler. 367: 879–890.

Deevska, G. M., K. A. Rozenova, N. V. Giltiay, M. A. Chambers, J. White, B. B. Boyanovsky, J. Wei, A. Daugherty, E. J. Smart, M. B. Reid, et al. 2009. Acid sphingomyelinase deficiency prevents diet-induced hepatic triacylglycerol accumulation and hyperglycemia in mice. J. Biol. Chem. 284: 8359–8368.

Duan, R., Y. Cheng, B. A. G. Jönsson, L. Ohlsson, A. Herbst, L. Hellström-Westas, and Å. Nilsson. 2007. Human meconium contains significant amounts of alkaline sphingomyelinase, neutral ceramidase, and sphingolipid metabolites. Pediatr. Res. 61: 61–66.

Duchateau, M. J., and H. Velthuis. 1989. Ovarian development and egg-laying in workers of *Bombus terrestris*. Entomol. Exp. Appl. 51: 199–213.

Gasteiger, E. A. H. C. 2005. Protein identification and analysis tools on the ExPASy server. Humana Press, Totowa, NJ.

Goni, F. M., and A. Alonso. 2002. Sphingomyelinases: enzymology and membrane activity. FEBS Lett. 531: 38–46.

Hall, T. A. 1999. BioEdit: a user-friendly biological sequence alignment editor and analysis program for Windows 95/98/NT. Nucleic Acids Symposium Series. 41: 95–98.

Han, L., S. He, J. Dong, Y. Wang, J. Huang, and J. Wu. 2017. First characterization of sphingomyeline phosphodiesterase expression in the bumblebee, *Bombus lantschouensis*. Sociobiology. 64: 85.

Hertervig, E., Å. Nilsson, R. D. Duan, J. Björk, and R. Hultkrantz. 1998. Alkaline sphingomyelinase activity is markedly decreased in familial

adenomatous polyposis and colorectal adenomas: a key factor to the unrestrained cell proliferation? Gastroenterology. 114: A610.

Hertervig, E., A. Nilsson, L. Nyberg, and R. D. Duan. 2015. Alkaline sphingomyelinase activity is decreased in human colorectal carcinoma. Cancer-Am. Cancer Soc. 79: 448–453.

Hofmann, K., S. Tomiuk, G. Wolff, and W. Stoffel. 2000. Cloning and characterization of the mammalian brain-specific, Mg2+-dependent neutral sphingomyelinase. Proc. Natl. Acad. Sci. USA 97: 5895–5900.

Kanfer, J. N., O. M. Young, D. Shapiro, and R. O. Brady. 1966. The metabolism of sphingomyelin. I. Purification and properties of a sphingomyelin-cleaving enzyme from rat liver tissue. J. Biol. Chem. 241: 1081–1084.

Kramer, M., S. Quickert, C. Sponholz, U. Menzel, K. Huse, M. Platzer, M. Bauer, and R. A. Claus. 2015. Alternative splicing of SMPD1 in human sepsis. PLoS One 10: e124503.

Li, S. C., S. Sonnino, G. Tettamanti, and Y. T. Li. 1988. Characterization of a nonspecific activator protein for the enzymatic hydrolysis of glycolipids. J. Biol. Chem. 263: 6588–6591.

Lim, S. M., K. Yeung, L. Trésaugues, T. H. Ling, and P. Nordlund. 2016. The structure and catalytic mechanism of human sphingomyelin phosphodiesterase like 3a–an acid sphingomyelinase homologue with a novel nucleotide hydrolase activity. FEBS J. 283: 1107–1123.

Liu, B., D. F. Hassler, G. K. Smith, K. Weaver, and Y. A. Hannun. 1998. Purification and characterization of a membrane bound neutral pH optimum magnesium-dependent and phosphatidylserine-stimulated sphingomyelinase from rat brain. J. Biol. Chem. 273: 34472–34479.

Livak, K. J., and T. D. Schmittgen. 2001. Analysis of relative gene expression data using real-time quantitative PCR and the 2(-Delta Delta C(T)) Method. Methods. 25: 402–408.

Matange, N., M. Podobnik, and S. S. Visweswariah. 2015. Metallophosphoesterases: structural fidelity with functional promiscuity. Biochem. J. 467: 201–216.

Munford, R. S., P. O. Sheppard, and P. J. O'Hara. 1995. Saposin-like proteins (SAPLIP) carry out diverse functions on a common backbone structure. J. Lipid Res. 36: 1653–1663.

O'Brien, N. W., N. M. Gellings, M. Guo, S. B. Barlow, C. C. Glembotski, and R. A. Sabbadini. 2003. Factor associated with neutral sphingomyelinase activation and its role in cardiac cell death. Circ. Res. 92: 589–591.

Petersen, T. N., S. Brunak, G. von Heijne, and H. Nielsen. 2011. SignalP 4.0: discriminating signal peptides from transmembrane regions. Nat. Methods 8: 785–786.

Ponting, C. P. 1994. Acid sphingomyelinase possesses a domain homologous to its activator proteins: saposins B and D. Protein Sci. 3: 359–361.

Rao, B. G., and M. W. Spence. 1976. Sphingomyelinase activity at pH 7.4 in human brain and a comparison to activity at pH 5.0. J. Lipid Res. 17: 506–515.

Renault, A. D., M. Starz-Gaiano, and R. Lehmann. 2002. Metabolism of sphingosine 1-phosphate and lysophosphatidic acid: a genome wide analysis of gene expression in Drosophila. Gene Expr. Patterns 2: 337–345.

Schneider, P. B., and E. P. Kennedy. 1967. Sphingomyelinase in normal human spleens and in spleens from subjects with Niemann-Pick disease. J. Lipid Res. 8: 202–209.

Schomburg, D. 2010. QMEAN: a comprehensive scoring function for model quality assessment. Proteins Structure Function & Bioinformatics. 71: 261–277.

Sjöqvist, U., E. Hertervig, A. Nilsson, R. D. Duan, A. Ost, B. Tribukait, and R. Löfberg. 2002. Chronic colitis is associated with a reduction of mucosal alkaline sphingomyelinase activity. Inflamm. Bowel Dis. 8: 258–263.

Tamura, K., G. Stecher, D. Peterson, A. Filipski, and S. Kumar. 2013. MEGA6: molecular evolutionary genetics analysis version 6.0. Mol. Biol. Evol. 30: 2725–2729.

Waterhouse, A., M. Bertoni, S. Bienert, G. Studer, G. Tauriello, R. Gumienny, F. T. Heer, T. A. P. de Beer, C. Rempfer, L. Bordoli, et al. 2018. SWISS-MODEL: homology modelling of protein structures and complexes. Nucleic Acids Res. 46: W296–W303.

Williams, N. H. 2004. Models for biological phosphoryl transfer. Biochim. Biophys. Acta 1697: 279–287.

Wu, J., Y. Shao, J. An, and J. Huang. 2007. Distribution and bionomics of *Bombus hypocrita* Pérez in north China. Apiculture of China. 58: 5–8.

Wu, J., J. An, J. Yao, J. Huang, and X. Feng. 2009. *Bombus* fauna (Hymenoptera, Apidae) in Hebei, China. Zoological Systematics. 34: 87–97.

Yong, J. K., S. Saeed, and M. J. Duchateau. 2003. Stimulation of colony initiation and colony development in *Bombus terrestris* by adding a male pupa: the influence of age and orientation. Apidologie. 34: 429–437.

Zinke, I., C. S. Schütz, J. D. Katzenberger, M. Bauer, and M. J. Pankratz. 2002. Nutrient control of gene expression in Drosophila: microarray analysis of starvation and sugar-dependent response. EMBO J. 21: 6162–6173.